

1 Title: **Hydrological Impacts of Mesquite Encroachment in the Upper San Pedro Watershed**

2 Authors: Wenming Nie, Yongping Yuan, William Kepner, Caroline Erickson, and Michael

3 Jackson

4 USEPA NERL, Landscape Ecology Branch, Environmental Sciences Division, 944 East Harmon

5 Avenue, Las Vegas, Nevada 89119 USA

6

7 Abstract

8 Over the past century, mesquite trees (*Prosopis spp.*) have exhibited substantial increase in
9 abundance throughout areas in the American Southwest that were once dominated by desert
10 grassland. To assess hydrological consequences of mesquite encroachment, the Soil and Water
11 Assessment Tool (SWAT) was applied to simulate progressive mesquite encroachments in the
12 upper San Pedro watershed (U.S./Mexico). The simulated average annual basin
13 evapotranspiration (ET) increases with mesquite encroachment, leading to the decrease of annual
14 water yield and percolation by 9.8% and 9.7%, respectively. Substantial increase of ET (up to
15 19.19 mm) and decrease of percolation, and surface runoff (to -12.90 and -3.20 mm, respectively)
16 were observed in the southeast, middle-west, and northern subwatersheds of the basin and the
17 most significant decrease of surface runoff (around -35.8%) was simulated during the wet period.
18 In addition, a non-linear hydrological response relative to mesquite encroachment was observed,
19 i.e. hydrological processes changed markedly until a certain amount (approximately 40%) of
20 grassland was removed, indicating that the strongest increase of ET occurred in the earliest
21 stages of encroachment. Consequently, changes in vegetation physiognomy, such as mesquite
22 encroachment, have broad implications for landuse management especially in regard to reliable
23 water supplies in arid and semi-arid environments.

1 Key Words: Mesquite Encroachment, Hydrological Response, ET, Runoff, San Pedro River,
2 Watershed Modeling, SWAT, Landscape Change

3

4 1. Introduction

5 Extensive encroachments of mesquite into grassland and savannas occurred throughout
6 the arid and semi-arid regions of the world over the last several decades or earlier (Briggs et al.,
7 2007; Goslee et al., 2003; Shiferaw et al., 2004; van Klinken et al., 2006). Two species of
8 mesquite tree, i.e. velvet mesquite (*Prosopis velutina*) and honey mesquite (*Prosopis*
9 *glandulosa*), have demonstrated significant expansion into the desert grasslands of the
10 Southwestern United States (Gassman et al., 2007). Most of the information regarding phase-
11 transition of desert grassland to indigenous mesquite woodland has been derived from anecdotal
12 accounts of rangeland users and managers or via the technique of repeat photography (Arnold et
13 al., 1998; Saleh et al., 2010; Stromberg et al., 1993; Wilcox et al., 2010). Regional change has
14 also been documented via satellite remote sensing (Kepner et al., 2002; Saleh et al., 2009). The
15 conversion of grassland into mesquite can generate many environmental consequences through
16 altering water and nutrient cycling, changing carbon storage, enhancing climate variability, and
17 reducing biodiversity (Ceballos et al., 2010; Jackson et al., 2002; Schlesinger et al., 1990; Zeng
18 et al., 1999). More specifically, considering that water is the limiting resource for the ecosystem
19 in semi-arid and arid regions, hydrological response to mesquite encroachment may directly
20 impact the availability of ecosystem services and consequently human well being. Impacts of
21 Land Use and Land Cover (LULC) change on hydrology in regions with mesquite encroachment
22 have been investigated (Hernandez et al., 2003; Miller et al., 2007; Nie et al., 2011; Saleh et al.,
23 2009; Stromberg et al., 1993). However, simultaneous changes in LULC, such as grassland

1 conversion to mesquite woodland and to urbanized areas increases the difficulty of quantifying
2 the effects of mesquite encroachment alone on hydrological cycling. To address this issue, a
3 series of land cover change scenarios were developed to represent progressive conversion of
4 grassland to mesquite woodland and the Soil and Water Assessment Tool (SWAT) model
5 (Arnold and Fohrer, 2005; Arnold et al., 1998; Gassman et al., 2007; Neitsch et al., 2005;
6 Srinivasan et al., 1998) was employed to simulate hydrological consequences of the developed
7 LULC scenarios. The objective of this study is to quantify how mesquite encroachment
8 influences the major hydrological processes at the basin scale. Although this study does not
9 provide explicit recommendations for resource managers, the intent is to contribute scientific
10 understanding that can be used toward environmental decision-making. This is especially relative
11 to the potential impact of landscape change on water provisioning, a vital ecosystem service in
12 the American Southwest.

13

14 2. Study Site

15 Extensive mesquite encroachment occurred in the upper San Pedro River basin from
16 1973 to 1986: proportional extent of mesquite increased from 2.81% to 14.33% and grassland
17 decreased from 41.07% to 35.00% (Saleh et al., 2009). The extensive vegetation change and
18 satellite documentation in this watershed makes it an ideal study site for the present research.

19 The upper San Pedro watershed originates in Sonora, Mexico near Cananea and flows
20 north into southeastern Arizona, USA (Figure 1). The drainage area for the upper San Pedro
21 watershed is approximately 7,400 km². Elevations in the watershed range from 900 to 2900
22 meters, and annual rainfall ranges from 300 to 750 mm (Kepner et al., 2000). The LULC in the

1 river basin includes woodland (oak and mesquite), desertscrub, grassland, forest, agriculture
2 crops, riparian, and urban (Saleh et al., 2009).

3

4 3. Method and Data

5 In this study, the SWAT model was calibrated and validated and then was used to
6 simulate a series of designed LULC scenarios, which represent progressive encroachment of
7 mesquite woodland into desert grassland. Hydrological consequences of mesquite encroachment
8 were evaluated by running the calibrated SWAT models with a constant Digital Elevation Model
9 (DEM), soil data, and meteorological forcing, while changing only the digital LULC data.

10 3.1 Model Description

11 The SWAT model is a continuous, long-term, physically based semi-distributed model
12 developed to assess impacts of climate and land management on hydrological processes,
13 sediment loading, and pollution transport in watersheds (Arnold et al., 1998). In the SWAT
14 model, a watershed is divided into subwatersheds or subbasins, which are further partitioned into
15 a series of hydrological response units (HRUs). HRUs are uniform units that share unique
16 combinations of soil and land use. Hydrological components, sediment yield, and nutrient cycles
17 are simulated for each HRU and then aggregated for the subbasins.

18 The hydrological cycle simulated in SWAT is based on the water balance equation:
19

$$20 \quad SW_t = SW_0 + \sum_{i=1}^t (R_{day} - Q_{surf} - E_a - w_{seep} - Q_{gw}) \quad (1)$$

21

22 where, SW_t and SW_0 are the final and initial soil water content on day i (mm H₂O), t the time
23 steps on day i , R_{day} the rainfall that reaches the soil surface on day i (mm), Q_{surf} the surface
24 runoff on day i (mm), E_a the evapotranspiration on day i (mm), w_{seep} the interflow on day i (mm),
25 and Q_{gw} is the baseflow on day i (mm) (Neitsch et al., 2005).

1 The simulated hydrological components include evapotranspiration (ET), surface runoff,
2 percolation, lateral flow, groundwater flow (return flow), transmission losses, ponds, and water
3 yield (Arnold et al., 1998). Evaporation and transpiration are simulated separately in SWAT:
4 evaporation is computed using exponential functions of soil depth and water content and
5 transpiration is estimated using a linear function of potential evapotranspiration (PET) and leaf
6 area index. Three methods can be used to estimate PET: Hargreaves (Hargreaves et al., 1985),
7 Priestley-Taylor (Priestley and Taylor, 1972), and Penman-Monteith (Monteith, 1965). The
8 Penman-Monteith method was used to calculate PET in this study. Surface runoff is simulated
9 using a modification of the Soil Conservation Service (now the Natural Resources Conservation
10 Service) Curve Number (SCS-CN) method (USDA, 1972) with daily rainfall. Curve number
11 values used for runoff estimation are based on soil type, LULC, and land management conditions
12 (Rallison and Miller, 1981) and are adjusted according to soil moisture conditions (Arnold et al.,
13 1993). Percolation is estimated using the combination of a storage routing technique and a crack-
14 flow model (Arnold et al., 1998). The lateral flow is estimated simultaneously with percolation
15 using a kinematic storage model (Solan et al., 1983). The groundwater flow (baseflow) into a
16 channel is calculated based on hydraulic conductivity of shallow aquifer, distance from subbasin
17 to main channel, and water table height (Hooghoudt, 1940). Transmission loss, amount of water
18 removed from tributary channels by transmission, is calculated using procedure described in SCS
19 Hydrology Handbook (Hibbert, 1983). Water yield, total amount of water leaving the HRU and
20 entering main channel, is equal to surface runoff plus lateral flow and baseflow, and minus
21 transmission loss and pond abstractions (Doorenbos and Pruitt, 1977).

22

23 3.2 Land Use and Land Cover Scenario Design

1 Mesquite encroachment occurred throughout the arid and semi-arid regions of the world
2 over the last several decades (Briggs et al., 2007; Goslee et al., 2003; Shiferaw et al., 2004; van
3 Klinken et al., 2006). To investigate hydrological impacts of mesquite encroachment, a series of
4 LULC change scenarios were developed with progressive conversion of mesquite from
5 grassland. These developed scenarios represent the trend of steady increase of the numbers of
6 polygons (patches), patch size, and the connectivity of mesquite woodland in the upper San
7 Pedro River basin identified by remote images (Kepner et al., 2002). Using the 1973 digital
8 LULC map developed via North American Landscape Characterization (NALC) project data
9 (Kepner et al., 2002) as a basis, gradual LULC changes were designed to simulate the patterns of
10 the past in the San Pedro (Kepner et al., 2002; Kepner et al., 2000) which provide predictive
11 inference (i.e. a change model) for evaluating projected trends. We considered 11 degrees of
12 change, including approximate 0, 10, 20, 30, 40, 50, 60, 70, 80, 90, and 100%, where 100% was
13 regarded as complete replacement of grassland with mesquite. In each step, the area of grassland
14 was reduced by approximate 10% to balance the expansion of mesquite, while the remainder of
15 the LULC remained unchanged.

16 The scenarios were developed by following procedure in ArcGIS: 1) extract mesquite and
17 grassland from 1973 digital LULC map, and reclassify grassland into mesquite (raster1, 100%
18 mesquite); 2) use “shrink” tool in GIS to obtain correct percentage of mesquite (10% - 50%); 3)
19 mosaic the derived raster using a raster with only grassland (reclassified from raster1 to a raster
20 with 0% mesquite); 4) since the shrink tool only works up to 50%, we used tool “expand” to
21 obtain correct percentages of mesquite for the rest of scenarios (60% - 90%).

22 3.3 Model Input Preparation

1 The basic SWAT model inputs include a DEM, soil data, LULC data, and meteorological
2 data. The DEM was derived from the National Elevation Dataset (NED) of USGS with 1 arc-
3 second resolution (Vadas et al., 2006), and the soil data was from the State Soil Geographic
4 (STATSGO) database. The LULC data of 1973, 1992 and 1997 used for this study was from the
5 NALC project (Landsat Multi-Spectral Scanner) and Landsat Thematic Mapper (Kepner et al.,
6 2002; Sharpley and William, 1990). For climate information, daily maximum and minimum
7 temperature, precipitation, solar radiation, relative humidity and wind speed are needed to
8 account for temporal variation in weather. This data can be historically measured, generated
9 using the SWAT built in WXGEN weather generator model (Sharpley and William, 1990), or
10 supplied to SWAT using a combination of the two methods. For this study, daily precipitation
11 and minimum-maximum temperature from Jan. 1960 to Apr. 2008 were acquired from the
12 National Climatic Data Center (NCDC). Twelve meteorological stations were found within or
13 nearby the upper San Pedro watershed (Fig. 1). Missing records of daily observations of
14 precipitation and minimum-maximum temperature were interpolated from weather data within a
15 radius of 25 miles using the method developed by Di Luzio et al. (2008). The remainder of the
16 weather information (solar radiation, relative humidity and wind speed) used in SWAT
17 simulation was generated by the WXGEN weather generator model (Sharpley and William,
18 1990).

19 The area for stream definition was set as 3500 ha, upon which the upper San Pedro River
20 basin was divided into 116 subbasins. The divided subbasins matched 12-digit HUCs in the
21 upper San Pedro watershed. The subbasins were further divided into HRUs based on the land
22 use, soil, and slope types (0.1%, 1%, and 5%). The number of HRUs differs when different
23 LULC maps are employed. As an example, the numbers of HRUs for 1992 and 1997 LULC are

1 2146 and 2225, respectively. There are 10 classes of LULC and 23 soil types in the upper San
2 Pedro watershed. Watershed parameterization includes the calculation of subbasin geometry
3 parameters from DEM and the assigning values to the HRUs through the inner database. The
4 database for the SWAT model includes parameter values for crops, urban, and soils, such as CN2
5 values (SCS runoff curve number for moisture condition II), SOL_AWC (Available water
6 capacity of the soil layer), LAI (leaf area index), and other soil physical and hydraulic properties.
7 Values were assigned to each HRU based on its LULC class and soil type during the
8 parameterization process. The simulation was initialized by setting default values of each
9 parameter; a five year warm up period was applied to erase the impact of initial condition for the
10 model calibration and validation.

11 3.4 Model Calibration and Validation

12 Simulations for model calibration were set up using 1992 NALC LULC data. Annual
13 (water year) and monthly streamflow from Oct. 1986 to Sept. 1995 at two USGS gages
14 (Redington and Charleston, Fig. 1) were used for model calibration. After model calibration,
15 simulations for model validation were set up using 1997 Landsat Thematic Mapper LULC data;
16 and annual (water year) and monthly streamflow at Tombstone (Oct. 1996 – Sept. 2005) and
17 Charleston (Oct. 1995 – Sept. 2005) were used for model validation. The model was calibrated
18 manually and three criteria were used to evaluate performance of model calibration/validation.

19 3.4.1 Manual calibration processes

20 The model was calibrated by manually editing sensitive parameters for hydrological components
21 (surface runoff, baseflow, lateral flow, ET, and channel transmission loss). In this study, the
22 lateral flow was assumed to be zero, because no obvious impervious layers in soil profiles, such
23 as black shales, which were pre-required for the lateral flow to be generated, were observed in

1 the watershed. In the SWAT model, the lateral flow was reduced to a very low level (close to
2 zero) by changing the adjust factor for lateral flow (Adjf_latq) from the default value of 1 into
3 0.02. Baseflow should be a very small portion recharging back to the stream because portions of
4 the upper San Pedro River are ephemeral stream. At the Redington gage (down- stream), river
5 only contains water during and immediately after a storm event and is dry the rest of the year. At
6 Tombstone and Charleston gage (upper-stream), although river flows intermittently, the water
7 supply may not be from baseflow for the relatively higher elevation (corresponding to deeper
8 groundwater table level values) than downstream. Thus, we eliminated the baseflow in the
9 SWAT model by reducing threshold water level in the shallow aquifer for re-evaporation
10 (Revapmn) and enhancing the re-evaporation coefficient and threshold water level in shallow
11 aquifer for baseflow (GWQMN). Surface runoff is the major water supply for the watershed.
12 Whereas, we noticed that streamflows were often under-estimated for light rainfall events and
13 over-estimated for large rainfall events. Woodward et al. (2002) found that runoff estimates
14 could be enhanced for relatively light rainfalls and be reduced for relative large rainfalls by
15 changing the initial abstraction ratio to be 0.05 from its originally defined value of 0.2. Thus, to
16 calibrate surface runoff, we set the initial abstraction ratio to be 0.05 and edited the CN2 (SCS
17 runoff curve number) to a relatively low value to match the change of initial abstraction ratio.
18 Channel transmission loss is a large portion (4% - 100%) of the water balance in the Walnut
19 Gulch Experimental Watershed, a sub-watershed of the upper San Pedro River basin (Sheffield
20 et al., 2009). USGS records show that monthly streamflow (in volume) at downstream locations
21 (Redington gage) is not always larger than in upperstream (Tombstone and Charleston gages),
22 indicating that transmission loss exist for the major channel (stream order 4 and 5). However, it's
23 hard to quantify the ratio of channel transmission loss to the basin recharge. In this study, we

1 assume approximately half of the water yield was lost through transmission loss during channel
2 routing processes. To calibrate the transmission loss, we set the TRNSRCH (Fraction of
3 transmission loss partitioned into deep aquifer) to be 1 and manually edit effective hydraulic
4 conductivity of channel (CH_K2). The optimal values for SWAT calibration were listed in
5 Table1.

6 3.4.2 Performance evaluation criteria

7 Three criteria were used to evaluate the model's performance on calibration and
8 validation: Nash-Sutcliff (NS) coefficient (Nash and Sutcliffe, 1970), coefficient of
9 determination (R^2), and percent bias (PBIAS) (Gupta et al., 1999). The calibration and validation
10 performance for the SWAT model is considered satisfactory when R^2 and NS are greater than 0.5
11 (Walvoord et al., 2003). When the absolute value of PBIAS is less than 15, the SWAT model is
12 rated a good performer (Walvoord et al., 2003).

13 3.4.3 Model application

14 After model calibration and validation, simulations were run for all developed LULC
15 scenarios with an unchanged DEM, soil data, and meteorological forcing from Jan. 1960 to Apr.
16 2008 (48.3 years) to evaluate hydrological consequences of mesquite encroachment in the upper
17 San Pedro watershed.

18

19 4. Results and Discussion

20 4.1 Calibration/Validation Results

21 The comparison between simulated and observed annual (in water year) and monthly
22 streamflow in the periods of calibration (Oct. 1986 – Sept. 1995) and validation (Oct. 1996 –
23 Sept. 2005) are shown in Figs. 2 and 3, respectively. In general, a good match can be seen

1 between simulated and observed values. The NS and R^2 values for the annual (in water year) and
2 monthly calibration and validation are listed in Table 2. All NS and R^2 values are above 0.5
3 (except NS coefficient for annual calibration at the Redington gage), and PBIAS are in the range
4 of $\pm 25\%$ (except annual calibration at the Charleston gage), suggesting satisfactory model
5 performance (Walvoord et al., 2003). Although the overall performance of the model is
6 satisfactory as shown in Figs. 2 and 3, and Table 2, a large difference was observed for the water
7 year of 1992 at Redington and 1993 at both Redington and Charleston. Intuitively, the simulated
8 values seem more reasonable because it matches the rainfall patterns as shown in Fig. 2. Possible
9 reasons for the discrepancies are the limitation of curve number method. First, high uncertainties
10 could be generated by using daily total rainfall depth as SWAT input. As an example, a large
11 amount of streamflow (4.21 mm) at the Redington gage on Aug. 1992 simulated in the SWAT
12 model was mainly attributed to a daily rainfall of 127.8 mm on Aug. 24, 1992 in the downstream.
13 Whereas, the rainfall depth at that day could be the combination of several relatively small
14 rainfall events, which may not be able to generate significant runoff (recorded streamflow in Aug.
15 1992 is 0.58 mm). Second, it fails to consider the effects of duration and intensity of
16 precipitation. For instance, runoff could be generated by some high-intensity, short-duration,
17 limited areal extent summer thunderstorms (Leuning et al., 2009) near observation gages.
18 Whereas, those limited areal extent summer thunderstorms may not be simulated by SWAT
19 model for a large extent.

20 Overall, the good match between simulation and observation, as well as high NS, R^2 , and
21 low absolute values for PBIAS indicates that streamflow can be described by the calibrated
22 model. Thus, the SWAT models set up by the optimal parameters were applied to evaluate
23 hydrological consequences to mesquite encroachments.

1 To further gain credence of the model, water balance was calculated for the calibration
2 and validation periods using equation 1. During the model calibration period (1986 – 1995), the
3 water balance errors were -0.29 mm to 0.73 mm, with relative errors (error/precipitation) from -
4 0.06 percent to 0.17 percent. During the model validation period (1996 – 2005), the absolute
5 water balance errors were -0.54 mm to 0.08 mm, with relative errors from -0.14 percent to 0.02
6 percent. The small errors suggest that the calibrated model satisfies the requirement of water
7 balance at the watershed scale.

8

9 4.2 Impacts of Mesquite Encroachment on Hydrology

10 Spatial and temporal impacts of mesquite encroachment on hydrology were investigated
11 through comparing variations of simulated hydrological processes between two extreme LULC
12 scenarios (with or without coverage of mesquite). Scenario 0 represents a LULC map with 0% of
13 grassland that was encroached by mesquite and Scenario 10 represents a LULC map with 100%
14 of grassland that was encroached by mesquite (Fig. 4). Fig. 5 shows the spatial distribution of
15 DEM, and deviations of four hydrological processes between Scenario 0 and Scenario 10.
16 Deviations were calculated as the difference between these two scenarios for each subbasin. As
17 an example, deviation of ET for subbasin 1 is the ET at subbasin 1 for Scenario 10 (all grassland
18 was replaced by mesquite) minus that for scenario 0. As shown in Fig. 5, most significant
19 variations of hydrological processes occurred in the southeast, middle-west, and northern
20 subwatersheds of the upper San Pedro River basin. An apparent increase of ET can be observed
21 in these subwatersheds, with an increase of annual averaged values up to 19.19 mm. In addition,
22 substantial decreases of annual averaged values of percolation and surface runoff were observed
23 in these subwatersheds, with a maximum decrease of -12.90 and -3.20 mm, respectively. Impacts

1 of mesquite encroachments on hydrology vary through time. Fig. 6 shows the relative decrease
2 of simulated basin annual surface runoff between Scenario 0 and Scenario 10 from 1960 to 2007.
3 Three multi-decadal precipitation regimes are identified in the upper San Pedro River Basin:
4 1960-1976, 1977-1994, and 1995-2007 (Fig. 6). A wet episode is sandwiched between two dry
5 conditions. The dry episodes in the upper San Pedro watershed are contemporaneous with
6 observed droughts of Arizona identified using an average of monthly records from 25 U.S.
7 historical climate network stations in Arizona from 1930 – 2002 (ADRW, 2010). As shown in
8 Fig. 6, the overall decreases of streamflow between Scenario 0 and Scenario 10 in wet periods -
9 are higher than the relative decreases during streamflow in dry periods which indicates that the
10 change of ET is higher in wet period. Therefore, precipitation is the secondary controlling factor
11 of ET besides LULC change. As we discussed in the model calibration section, streamflow was
12 mainly composed of surface runoff. The runoff was simulated using SCS Curve Number method
13 in the SWAT model. Compared to grassland, mesquite is associated with a relatively smaller
14 curve number. Theoretically, the differences between simulated runoffs for grassland and
15 mesquite increase with increasing rainfall (NRCS, 1997). Thus, deviations in simulated annual
16 surface runoff between the two scenarios during the wet period will be higher than those in dry
17 episode, leading to higher deviation in annual streamflow during the wet period.

18 Impacts of mesquite encroachments on hydrological processes were related to
19 meteorological forcing and some geographical properties, including area, elevation and slope. As
20 shown in Table 3, positive correlations between ET and elevation or precipitation were observed,
21 suggesting spatial distribution of elevation or precipitation is the secondary controlling factor of
22 ET besides LULC change. The positive correlation could be due to more water available for
23 evapotranspiration. In addition, negative correlations between other hydrological processes and

1 elevation or precipitation were examined. The negative correlation could also be related to the
2 water availability, i.e. when more rainfall is applied in the upper San Pedro watershed, more
3 significant changes (decreases) in surface runoff, percolation, and water yield should be
4 simulated.

5 The relationship among three major hydrological processes (runoff, ET, and percolation)
6 and percentage of grassland removed in the upper San Pedro River basin are plotted in Figs. 7
7 and 8. It shows that complete replacement of grassland with mesquite increases the simulated
8 annual averaged basin ET from 384.3 to 386.1 mm and decreases the annual averaged basin
9 runoff amount from 2.66 to 2.35 mm. Full encroachment of mesquite into grassland reduces
10 annual averaged basin percolation from 13.35 to 12.05 mm. The change of basin annual
11 averaged values of ET, percolation, and surface runoff are not substantial (few millimeters).
12 However, considering the effects of spatial heterogeneity and weather condition (wet versus dry),
13 impacts of mesquite encroachments on hydrology could still be significant for subwatersheds
14 with more mesquite encroachments in wet periods.

15 The increased ET with mesquite encroachment can be attributed to the higher
16 transpiration demand of mesquite relative to grassland. The quantification of ET for different
17 riparian species in the upper San Pedro River basin suggested that mesquite woodlands have
18 much higher annual ET rates than grasslands (Scott et al., 2006). Unlike the shallow rooted
19 grassland, mesquite has a shallow lateral root system and a deep vertical root system, which
20 enables it to use water in shallow and deep soils, as well as in the groundwater system
21 (Heitschmidt et al., 1988; Scott et al., 2006). This ability enhances the capacity of mesquite to
22 compete for water with grassland and other shallow-rooted plants in subbasins with a shallow
23 water table, such as riparian settings. In uplands, studies also show that water yield of rangeland

1 could be significantly increased through controlling brush, such as honey mesquite (Hibbert,
2 1983). It was indicated that ET of the mesquite treated watershed was significantly lower than
3 ET of the nearby non-treated one (10% - 17%) in the North Concho River watershed near San
4 Angelo, Texas, especially during growing seasons (Saleh et al., 2009). The increase of ET
5 changes the water balance, leading to less water to percolate through the bottom of soil and
6 consequently decreasing groundwater supply.

7 The higher ET due to mesquite encroachment can also impact the volume of surface
8 runoff. Given that more precipitation evapotranspired, less moisture would remain in the soil
9 after rainfall events, resulting in higher demand of water to saturate the top soil layers before
10 generating any runoff in the next rainfall event. In the SWAT model, the value of Curve Number
11 is justified based on antecedent soil moisture condition before surface runoff is calculated.
12 Consequently, less runoff could be expected with higher ET due to mesquite encroachment into
13 grassland.

14 A noticeable non-linear response of hydrology to grassland removal can be observed, i.e.
15 hydrological processes changed markedly until a certain amount of grassland was removed (Figs.
16 7 and 8). For example, the decrease of water yield before a certain percentage (approximately
17 40%, estimated by the switch of the slope from -0.005 to -0.001) of grassland was removed is
18 much faster than after (). Thus, the certain percentage of grassland removal is a threshold of
19 water yield responses to mesquite encroachment. The sensitivity of hydrological responses to
20 landscape change rapidly decreases when the percentage grassland removal exceeds a certain
21 amount (a threshold). It indicates that the strongest response of hydrology to grassland removal
22 occurred in the earliest stage of mesquite encroachment.

1 The non-linear relationship between hydrology and landscape change was also observed
2 by other researchers (Ghaffari et al., 2010; Li et al., 2007; Zehe and Sivapalan, 2009). The
3 slower hydrological responses in the second stage of mesquite encroachment (after a certain
4 amount of grassland removal) are probably because the evapotranspiration has reached its
5 maximum capacity. The ration of ET over total precipitation (rainfall and snowmelt) is 95.4%
6 when a certain amount of grassland was replaced by mesquite. Although the evapotranspiration
7 capability increases with mesquite encroachment, presumably because of its higher leaf area
8 index, the actual amount of transpired water does not greatly increase because of the limited
9 available water for transpiration.

10

11 5. Summary and Conclusions

12 Progressive encroachments of mesquite into grassland from 0 – 100% were simulated
13 using the SWAT model for the upper San Pedro watershed to investigate hydrological
14 consequences of mesquite encroachment in a semiarid system. The simulation results show that
15 the annual average basin ET increases with the removal of grassland, while surface runoff and
16 percolation decreases with mesquite encroachment. Impacts of mesquite encroachment on
17 hydrology are more significant for subwatersheds with more grassland replaced by mesquite
18 during wet periods. Notably, simulation results also indicate a non-linear relationship between
19 hydrological response and mesquite encroachment, i.e. the impact on the simulated hydrological
20 processes is significant when grassland removal is below a threshold.

21 An increase of ET will lead to the decrease of the local or regional water supply because
22 the total amount of water supply (the sum of surface water and groundwater flow) is equal to
23 precipitation (including snow melt) minus ET. In this study, although only a 1.8 mm increase of

1 annual average basin ET was simulated when grassland was fully replaced by mesquite in the
2 upper San Pedro Watershed, the simulated total runoff (water yield) and percolation decreased
3 by 9.8% and 9.7%, respectively. In addition, a substantial increase in ET (up to 19.19 mm) and
4 decrease of percolation and surface runoff (to -12.90 and -3.20 mm, respectively) were observed
5 in the southeast, middle-west, and northern subwatersheds. The most significant decrease of
6 surface runoff (around 35.8%) was simulated during wet periods. The increase of ET in the arid
7 or semiarid regions is likely to develop a positive feedback that will reinforce the encroachment
8 of mesquite into grassland. When the replacement of grassland by mesquite begins, less soil
9 moisture is available for the ecosystem because the transpiration by mesquite is much higher
10 than grassland. The non-linear relationship between mesquite encroachment and hydrological
11 response indicates that the strongest increase of ET occurred in the early stages of encroachment.

12 The work associated with this study was intended to provide information to land
13 managers concerned about future ecosystem condition within the context of a large watershed. It
14 was especially focused at issues related to hydrological response as a consequence of potential
15 vegetation change scenarios. Clearly, retrospective analysis using remote sensing has
16 documented that woody plants, such as mesquite, are replacing native desert grasses as the
17 dominant life form. Historically, land managers have engaged in woody plant control activities,
18 e.g. controlled fires, herbicide treatments, and mechanical manipulation, however the most
19 impact can be realized if such actions are engaged during the earliest stages of encroachment.

20 **Acknowledgement**

21
22 The authors are grateful for the valuable inputs and suggestions provided by the associate editor
23 and anonymous reviewers. Although this work was reviewed by USEPA and approved for
24 publication, it may not necessarily reflect official Agency policy. Mention of trade names or
25 commercial products does not constitute endorsement or recommendation for use.

26
27 6. References

1 ADRW, 2010. Arizona Water Atlas, Volume 1, Appendix E: Arizona Climate and Drought.

2 Arnold, J.G., Allen, P.M., Bernhardt, G., 1993. A Comprehensive Surface-Groundwater Flow
3 Model. *J Hydrol* 142, 47-69.

4 Arnold, J.G., Fohrer, N., 2005. SWAT2000: current capabilities and research opportunities in
5 applied watershed modelling. *Hydrol Process* 19, 563-572.

6 Arnold, J.G., Srinivasan, R., Muttiah, R.S., Williams, J.R., 1998. Large area hydrologic
7 modeling and assessment - Part 1: Model development. *J Am Water Resour As* 34, 73-89.

8 Briggs, J.M., Schaafsma, H., Trenkov, D., 2007. Woody vegetation expansion in a desert
9 grassland: Prehistoric human impact? *J Arid Environ* 69, 458-472.

10 Ceballos, G., Davidson, A., List, R., Pacheco, J., Manzano-Fischer, P., Santos-Barrera, G.,
11 Cruzado, J., 2010. Rapid Decline of a Grassland System and Its Ecological and Conservation
12 Implications. *Plos One* 5, -.

13 Doorenbos, J., Pruitt, W.O., 1977. Guidelines for prediction of crop water requirements. FAO
14 Irrig. and Drain. Paper No. 24 (revised). Rome, Italy: United Nations FAO.

15 Gassman, P.W., Reyes, M.R., Green, C.H., Arnold, J.G., 2007. The soil and water assessment
16 tool: Historical development, applications, and future research directions. *T Asabe* 50, 1211-
17 1250.

18 Ghaffari, G., Keesstra, S., Ghodousi, J., Ahmadi, H., 2010. SWAT-simulated hydrological
19 impact of land-use change in the Zanjanrood Basin, Northwest Iran. *Hydrol Process* 24, 892-903.

20 Goslee, S.C., Havstad, K.M., Peters, D.P.C., Rango, A., Schlesinger, W.H., 2003. High-
21 resolution images reveal rate and pattern of shrub encroachment over six decades in New
22 Mexico, USA. *J Arid Environ* 54, 755-767.

23 Gupta, H.V., Sorooshian, S., Yapo, P.O., 1999. Status of Automatic Calibration for Hydrologic
24 Models: Comparison with Multilevel Expert Calibration. *J Hydrol Eng* 4, 135-143.

25 Hargreaves, G.L., Hargreaves, G.H., Riley, J.P., 1985. Agricultural Benefits for Senegal River
26 Basin. *J Irrig Drain E-Asce* 111, 113-124.

27 Heitschmidt, R.K., Ansley, R.J., Dowhower, S.L., Jacoby, P.W., Price, D.L., 1988. Some
28 Observations from the Excavation of Honey Mesquite Root Systems. *J Range Manage* 41, 227-
29 231.

30 Hernandez, M., Kepner, W.G., Semmens, D.J., W., E.D., Goodrich, D.C., Miller, R.C., 2003.
31 Integrating a Landscape/Hydrologic Analysis for Watershed Assessment, The First Interagency
32 Conference on Research in the Watersheds, pp. 1-6.

33 Hibbert, A.R., 1983. Water Yield Improvement Potential by Vegetation Management on Western
34 Rangelands. *Water Resour Bull* 19, 375-381.

35 Hooghoudt, S.B., 1940. Bijdrage tot de kennis van enige natuurkundige grootheden van de
36 grond. *Versl. Landbouwk. Onderz.* 46, 515-707.

37 Jackson, R.B., Banner, J.L., Jobbagy, E.G., Pockman, W.T., Wall, D.H., 2002. Ecosystem
38 carbon loss with woody plant invasion of grasslands. *Nature* 418, 623-626.

39 Kepner, Edmonds, C.M., Watts, C.J., 2002. Remote Sensing and Geographic Information
40 Systems for Decision Analysis in Public Resource Administration: A Case Study of 25 Years of
41 Landscape Change in a Southwestern Watershed., 31. U.S. Environmental Protection Agency,
42 EPA/600/R-02/039.

43 Kepner, W., Watts, C.J., Edmonds, C.M., Maingi, J.K., Marsh, S.E., Luna, G., 2000. Landscape
44 approach for detecting and evaluating change in a semiarid environment. *Environ Monit Assess*
45 64, 179-195.

1 Leuning, R., Zhang, Y.Q., Rajaud, A., Cleugh, H., Tu, K., 2009. A simple surface conductance
2 model to estimate regional evaporation using MODIS leaf area index and the Penman-Monteith
3 equation (vol 45, W10419, 2008). *Water Resour Res* 45, -.

4 Li, K.Y., Coe, M.T., Ramankutty, N., De Jong, R., 2007. Modeling the hydrological impact of
5 land-use change in West Africa. *J Hydrol* 337, 258-268.

6 Miller, S.N., Guertin, D.P., Goodrich, D.C., 2007. Hydrologic modeling uncertainty resulting
7 from land cover misclassification. *J Am Water Resour As* 43, 1065-1075.

8 Monteith, J.L., 1965. *Evaporation and environment*, 19th Symposia of the Society for
9 Experimental Biology. Cambridge University, London, U.K., pp. 205-234.

10 Nash, J.E., Sutcliffe, J.V., 1970. River flow forecasting through conceptual models. Part I: a
11 discussion of principles. *J Hydrol*, 282-290.

12 Neitsch, S.L., Arnold, J.G., Kiniry, J.R., Williams, J.R., 2005. *Soil and Water Assessment Tool*.
13 Theoretical Documentation. Version 2005, Temple, TX.

14 Nie, W., Yuan, Y., Kepner, W., Nash, M.S., Jackson, M., Erickson, C., 2011. Assessing impacts
15 of Landuse and Landcover changes on hydrology for the upper San Pedro watershed. *J Hydrol*, 1
16 - 10.

17 NRCS, 1997. Part 630 - Hydrology, *National Engineering Handbook*. Washington D.C.

18 Priestley, C., Taylor, R.J., 1972. Assessment of Surface Heat-Flux and Evaporation Using Large-
19 Scale Parameters. *Mon Weather Rev* 100, 81-82.

20 Rallison, R.E., Miller, N., 1981. Past, Present and future SCS runoff procedure. *Water Resources*
21 *Publication*, Littleton, CO.

22 Saleh, A., Brown, C.S., Teagarden, F.M., McWilliams, S.M., Hauck, L.M., 2010. Response to
23 commentary on "Effect of brush control on evapotranspiration in the North Concho River
24 watershed using the eddy covariance technique" by Wilcox et al. (2010). *J Soil Water Conserv*
25 65, 85a-86a.

26 Saleh, A., Wu, H., Brown, C.S., Teagarden, F.M., McWilliams, S.M., Hauck, L.M., Millican,
27 J.S., 2009. Effect of brush control on evapotranspiration in the North Concho River watershed
28 using the eddy covariance technique. *J Soil Water Conserv* 64, 336-349.

29 Schlesinger, W.H., Reynolds, J.F., Cunningham, G.L., Huenneke, L.F., Jarrell, W.M., Virginia,
30 R.A., Whitford, W.G., 1990. Biological Feedbacks in Global Desertification. *Science* 247, 1043-
31 1048.

32 Scott, R.L., Goodrich, D., Levick, L., 2006. Determining the riparian groundwater use within the
33 San Pedro Riparian National Conservation Area and the Sierra Vista Subwatershed, Arizona. In
34 *Hydrologic Requirements of and Consumptive Ground-Water Use by Riparian Vegetation along*
35 *the San Pedro River, Arizona*, in: J.M. Leenhouts, J.C.S., and R.L. Scott, (Ed.), *USGS Sci.*
36 *Invest. Report* 2005, pp. 107-152.

37 Sharpley, A.N., William, J.R., 1990. *EPIC-Erosion/Productivity Impact Calculator: I -- model*
38 *documentation*. U.S. Department of Agriculture Tech. Bull.

39 Sheffield, J., Ferguson, C.R., Troy, T.J., Wood, E.F., McCabe, M.F., 2009. Closing the terrestrial
40 water budget from satellite remote sensing. *Geophys Res Lett* 36, -.

41 Shiferaw, H., Teketay, D., Nemomissa, S., Assefa, F., 2004. Some biological characteristics that
42 foster the invasion of *Prosopis juliflora* (Sw.) DC. at Middle Awash Rift Valley Area, north-
43 eastern Ethiopia. *J Arid Environ* 58, 135-154.

44 Solan, P.G., Morre, I.D., Coltharp, G.B., Eigel, J.D., 1983. Modeling surface and subsurface
45 stormflow on steeply-sloping forested watersheds. *Water Resource Inst. Report* 142. University
46 of Kentucky, Lexington.

1 Srinivasan, R., Ramanarayanan, T.S., Arnold, J.G., Bednarz, S.T., 1998. Large area hydrologic
2 modeling and assessment - Part II: Model application. *J Am Water Resour As* 34, 91-101.
3 Stromberg, J.C., Wilkins, S.D., Tress, J.A., 1993. Vegetation-Hydrology Models - Implications
4 for Management of Prosopis-Velutina (Velvet Mesquite) Riparian Ecosystems. *Ecol Appl* 3,
5 307-314.
6 USDA, S.C.S., 1972. National Engineering Handbook Section 4 Hydrology.
7 Vadas, P.A., Krogstad, T., Sharpley, A.N., 2006. Modeling phosphorus transfer between labile
8 and nonlabile soil pools: Updating the EPIC model. *Soil Sci Soc Am J* 70, 736-743.
9 van Klinken, R.D., Graham, J., Flack, L.K., 2006. Population ecology of hybrid mesquite
10 (Prosopis species) in Western Australia: how does it differ from native range invasions and what
11 are the implications for impacts and management? *Biol Invasions* 8, 727-741.
12 Walvoord, M.A., Phillips, F.M., Stonestrom, D.A., Evans, R.D., Hartsough, P.C., Newman,
13 B.D., Striegl, R.G., 2003. A reservoir of nitrate beneath desert soils. *Science* 302, 1021-1024.
14 Wilcox, B.P., Walker, J.W., Heilman, J.L., 2010. Commentary on "Effect of brush control on
15 evapotranspiration in the North Concho River watershed using the eddy covariance technique"
16 by Saleh et al. (2009). *J Soil Water Conserv* 65, 83a-84a.
17 Zehe, E., Sivapalan, M., 2009. Threshold behaviour in hydrological systems as (human) geo-
18 ecosystems: manifestations, controls, implications. *Hydrol Earth Syst Sc* 13, 1273-1297.
19 Zeng, N., Neelin, J.D., Lau, K.M., Tucker, C.J., 1999. Enhancement of interdecadal climate
20 variability in the Sahel by vegetation interaction. *Science* 286, 1537-1540.
21
22

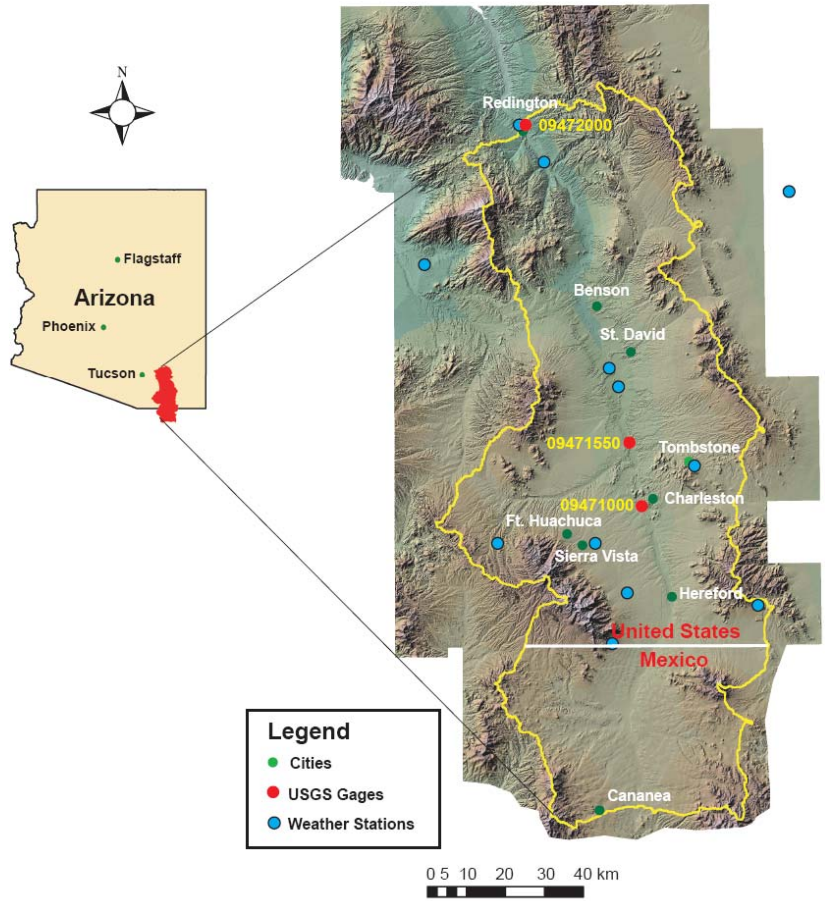


Fig.1. Locations of rural and municipal areas, USGS monitoring gages, and weather stations in the upper San Pedro watershed (modified from Kepner et al., 2000)

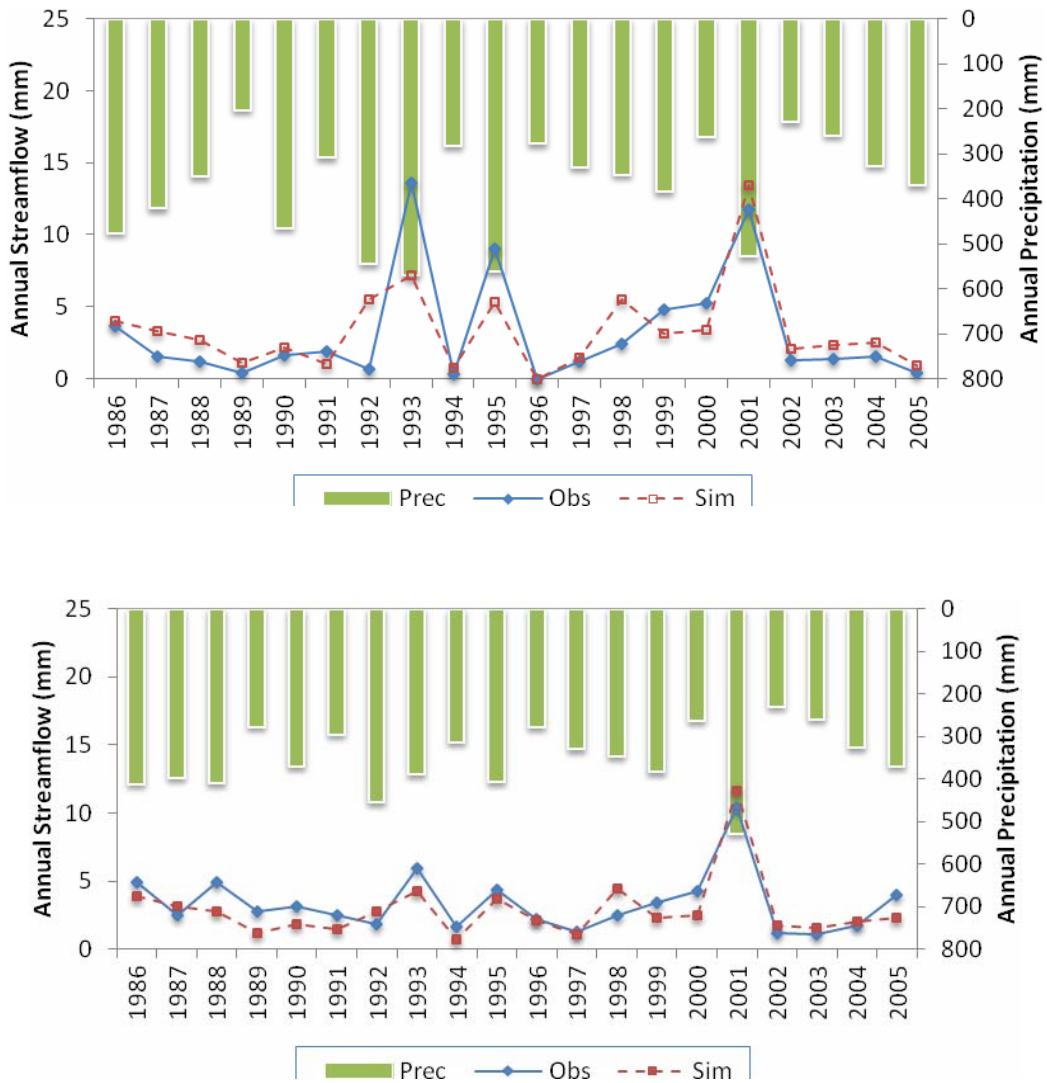


Fig. 2. Annual (in water year) precipitation and simulated and observed streamflow in the upper San Pedro Watershed. Upper: Redington (1986 – 1995) and Tombstone (1997 – 2005) gages; Lower: Charleston gage (1986 – 2005).

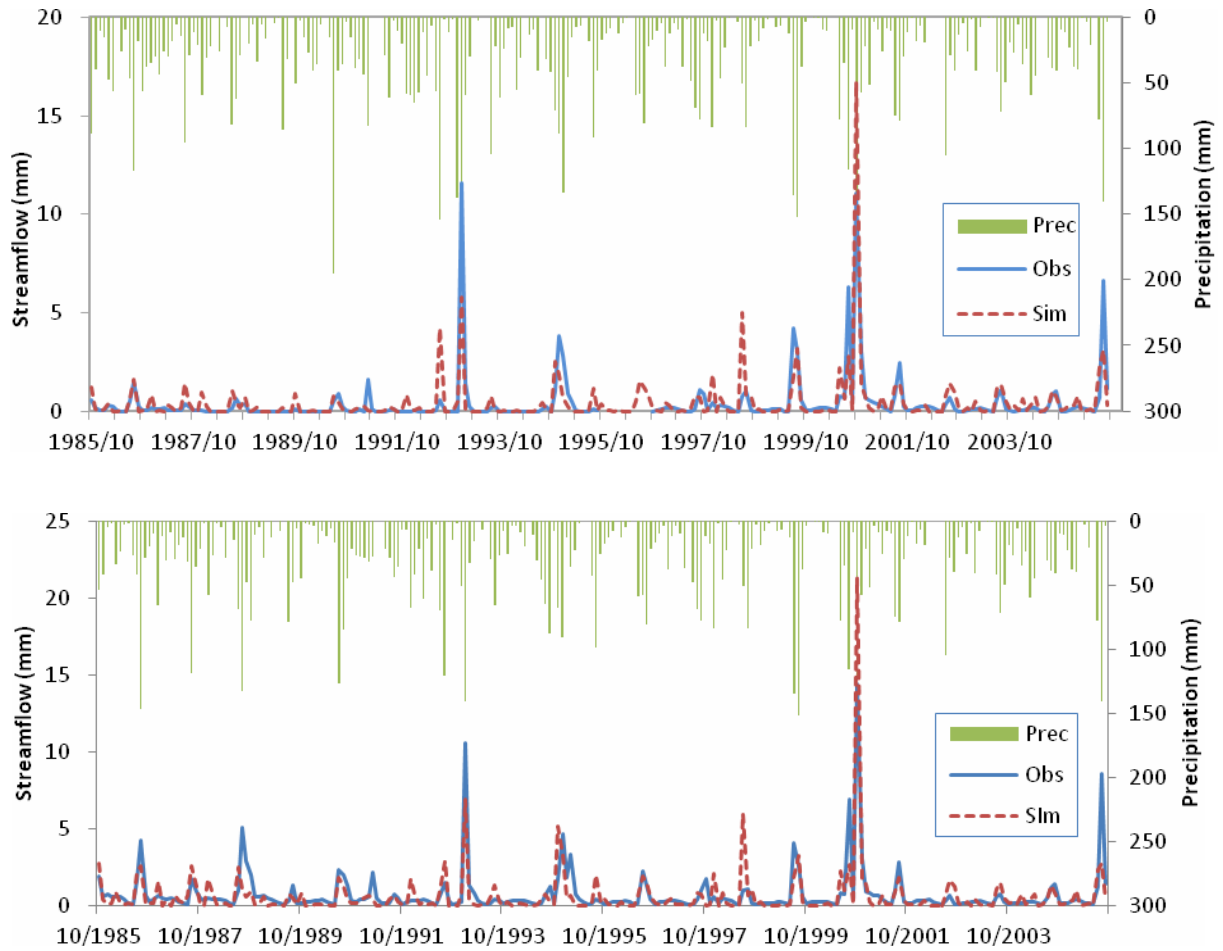


Fig. 3. Monthly precipitation and simulated and observed streamflow in the upper San Pedro watershed. Upper: Redington (10/1985-09/1995) and Tombstone (10/1996-09/2005) gages; Lower: Charleston gage (10/1985-09/2005).

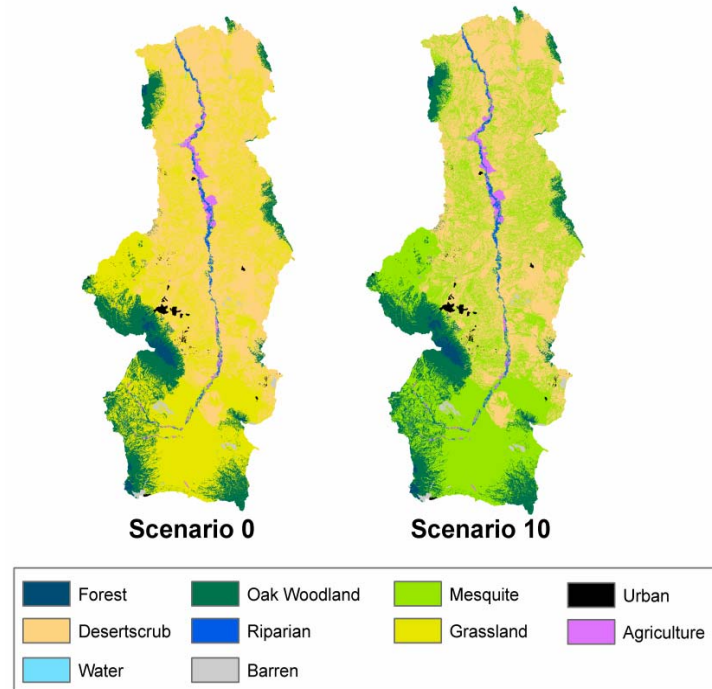


Fig. 4. Two Land Use and Land Cover scenarios in the Upper San Pedro Watershed. Scenario 0: 0% of grassland was replaced by mesquite; Scenario 10: 100% of grassland was replaced by mesquite.

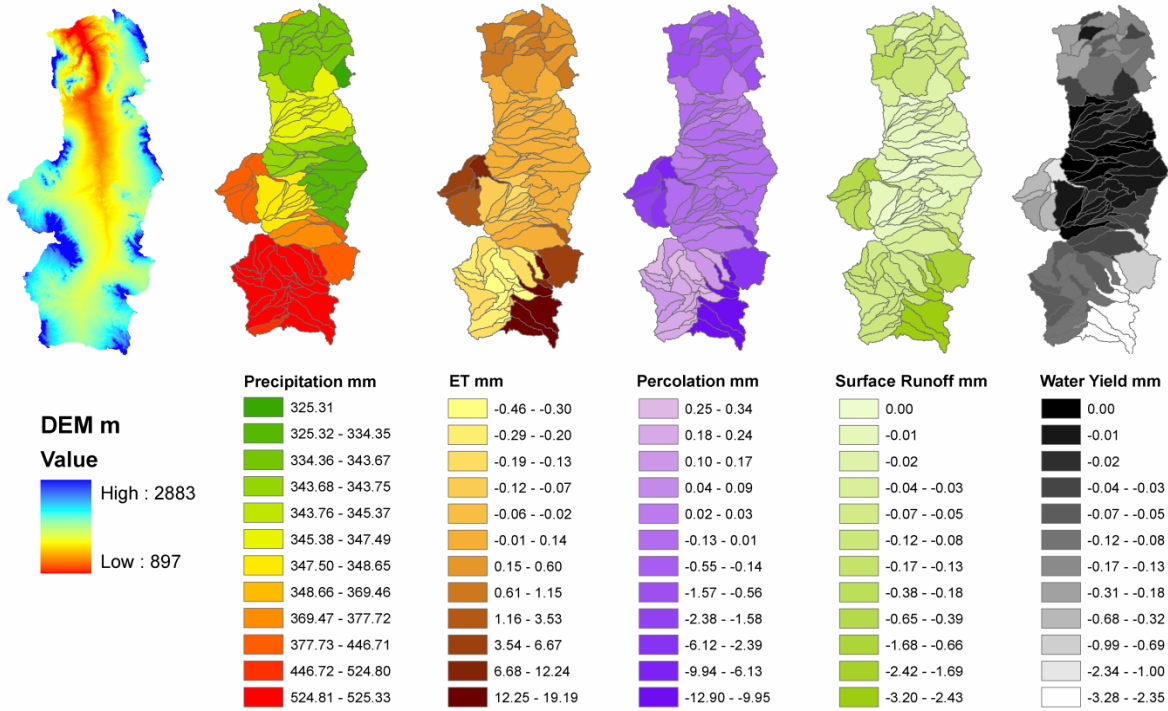


Fig. 5. Spatial distribution of DEM, precipitation, and deviation of four hydrological processes between land use/ land cover Scenario 0 (0% of grassland was replaced by mesquite) and Scenario 10 (100% of grassland was replaced by mesquite).

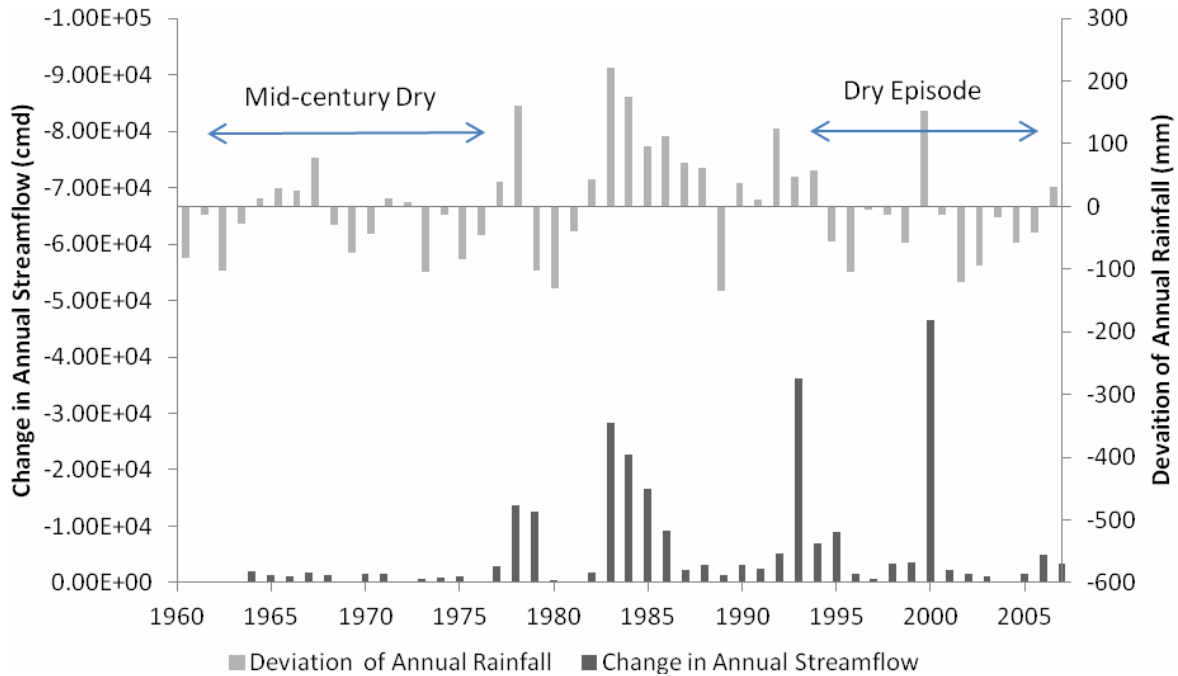


Fig. 6. Relative decrease of simulated annual streamflow in cubic meter per year (between Scenario 0 and Scenario 10) and deviation of annual rainfall from 1960 to 2007. The dry episodes in the upper San Pedro watershed are contemporaneous with observed droughts of Arizona identified using average of monthly records from 25 U.S. historical climate network stations in Arizona (ADRW, 2010).

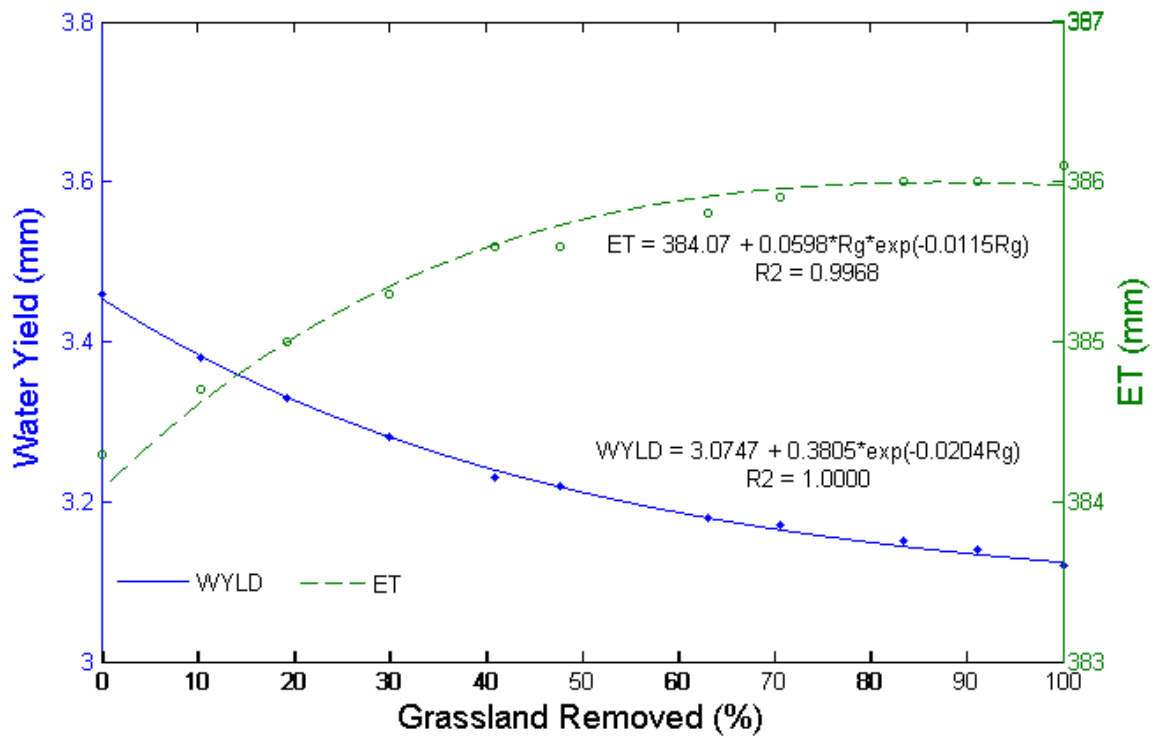


Fig. 7. Water yield and ET plotted against percentage of grassland removed (Rg) for the period from 1960 to 2008 based on progressive encroachment of mesquite scenarios.

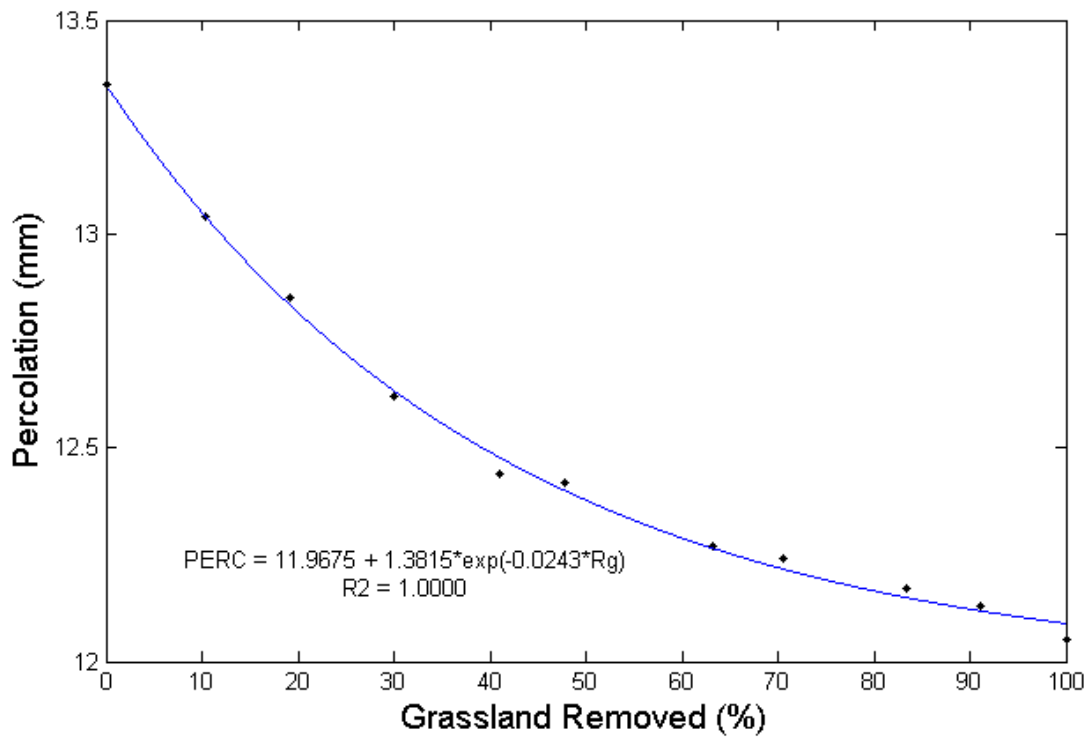


Fig. 8. Precolation (PERC) plotted against percentage of grassland removed (Rg) for the period from 1960 to 2008 based on progressive encroachment of mesquite scenarios.

Table 1. Description, default and calibrated values that were used in the model calibration/validation (*, the multiple sign, means the default values of parameter are multiplied by the number following the “*”).

Parameter	Default	Description	Calibrated Value
Adjf_latq	1	Adjust factor for lateral flow	0.02
λ	0.2	Initial Abstraction Ratio	0.05
CN2	30-92	SCS runoff curve number for moisture condition II	*0.58
ESCO	0.95	Soil evaporation compensation factor	0.05
SOL_AWC	0.01-0.19	Available water capacity of the soil layer	*1.4
GW_Revap	0.02	Revaporation coefficient	0.2
Revapmn	1	Threshold water level in shallow aquifer for revap	0
GWQMN	0	Threshold water level in shallow aquifer for baseflow	100
TRNSRCH	0	Fraction of transmission loss partitioned into deep aquifer	1
CH_K2	0	Effective hydraulic conductivity of channel	0.6

Table 2. Criteria for examining the accuracy of calibration and validation (the validation period at Tombstone gage is from Oct. 1996 to Sept. 2005).

Index	Calibration (10/1985 - 09/1995)				Validation (10/1995 - 09/2005)			
	Redington		Charleston		Tombstone		Charleston	
	Yearly	Monthly	Yearly	Monthly	Yearly	Monthly	Yearly	Monthly
NS Coefficient	0.45	0.56	0.82	0.52	0.94	0.57	0.93	0.55
R ²	0.66	0.57	0.66	0.55	0.84	0.70	0.82	0.70
PBIAS	1.94	-1.29	25.46	24.63	-16.27	-9.23	1.38	3.00

Table 3 Pair-wise Pearson correlation for four physical parameters (Area, elevation, slope, and precipitation) and changes of four hydrological processes (ET, percolation, surface runoff, and water yield) between land use/ land cover Scenario 0 (0% of grassland was replaced by mesquite) and Scenario 10 (100% of grassland was replaced by mesquite).

	Area	Elevation	Slope	PRECIP	ET	PERC	SURQ	WYLD
Area	1.00							
Elevation	0.23	1.00						
Slope	0.29	0.14	1.00					
PRECIP	0.00	0.60	-0.21	1.00				
ET	0.16	0.31	0.07	0.37	1.00			
PERC	-0.15	-0.30	-0.08	-0.36	-1.00	1.00		
SURQ	-0.17	-0.31	-0.02	-0.43	-0.98	0.98	1.00	
WYLD	-0.16	-0.32	-0.06	-0.42	-0.98	0.99	0.99	1.00

n = 116, bold numbers are for p<0.05